

Sharing pattern submodels for prediction with missing values

Lena Stempfle, Fredrik Johansson

Department of Computer Science and Engineering (CSE), Chalmers
University of Technology, Sweden
stempfle@chalmers.se fredrik.johansson@chalmers.se

Abstract

Missing values are unavoidable in many applications of machine learning and present a challenge both during training and at test time. When variables are missing in recurring patterns, fitting separate pattern submodels have been proposed as a solution. However, independent models do not make efficient use of all available data. Conversely, fitting a shared model to the full data set typically relies on imputation which may be suboptimal when missingness depends on unobserved factors. We propose an alternative approach, called sharing pattern submodels, which make predictions that are a) robust to missing values at test time, b) maintains or improves the predictive power of pattern submodels, and c) has a short description enabling improved interpretability. We identify cases where sharing is provably optimal, even when missingness itself is predictive and when the prediction target depends on unobserved variables. Classification and regression experiments on synthetic data and two healthcare data sets demonstrate that our models achieve a favorable trade-off between pattern specialization and information sharing.

1 Introduction

Machine learning models are often used in settings where model inputs are partially missing either during training or at the time of prediction (Rubin, 1976; Schafer and Graham, 2002). If not handled appropriately, missing values can lead to increased bias or to models that are unapplicable in deployment (Liu et al., 2020; Le Morvan et al., 2020) without imputing the values of unobserved variables.

When missingness is dependent on unobserved factors that are related also to the prediction target, the fact that a variable is unmeasured can itself be predictive—so-called *informative missingness* (Rubin, 1976; Marlin, 2008). This is particularly prevalent in healthcare applications (Janssen et al., 2009; Che et al., 2018). In such cases, imputation of missing values is often insufficient, and it can be beneficial to let models make predictions based on both the partially observed data and on indicators for which variables are missing (Jones, 1996; Groenwold et al., 2012). As mentioned in Morvan et al. (2020), even the linear model—the simplest of all regression models—has not yet been thoroughly investigated with missing values and still reveals unexpected challenges.

Pattern missingness emerges in data generating processes where there are structural reasons for which variables are measured—samples are grouped by recurring patterns of measured and missing variables (Little, 1993). In Figure 1, we illustrate an example of this when observing patients from three different clinics, each systematically collecting slightly different measurements. *Pattern submodels* have been proposed for this setting, fitting a separate model to samples from each pattern (Fletcher Mercaldo and Blume, 2020; Marshall et al., 2002). This solution

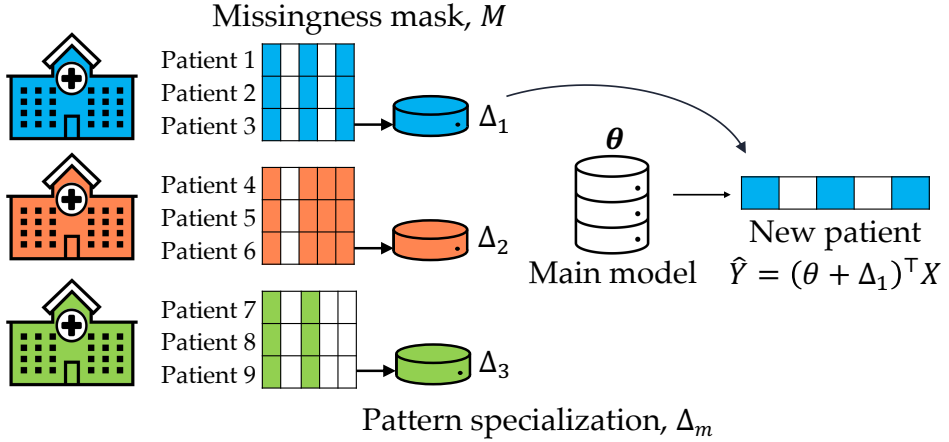


Figure 1: Coefficient sharing between a main model θ and pattern submodels for three clinics with different patterns in missing values. Without specialization Δ_m , an average prediction shared by clinics with different patterns may not lead to an optimal solution for any of them. Conversely, fitting separate models for each clinic does not use all of the available data efficiently and leads to high variance.

does not rely on imputation and can improve interpretability over black-box methods (Rudin, 2019), but can suffer from high variance, especially when the number of distinct patterns is large and the number of samples for a given pattern is small. Moreover, if the fitted models differ significantly between patterns, it may be hard to compare or sanity-check their predictions. Notably, pattern submodels disregard the fact that the prediction task is shared between each pattern.

We propose the *sharing pattern submodel* (SPSM) in which submodels for different missingness patterns share coefficients while allowed limited specialization. This encourages efficient use of information across submodels leading to a beneficial tradeoff between predictive power and variance in the case where similar submodels are desired and sample sizes per pattern are small. Models with few and small differences between patterns are easier to describe and interpret by domain experts.

We describe SPSM and present a running example to illustrate our idea in Section 3. Next, we prove that in linear-Gaussian data generating processes, coefficient sharing *does not introduce additional bias*—even when the prediction target depends on partially missing variables and on the missingness pattern (Section 4). Finally, we find in an experimental evaluation on real-world and synthetic data that SPSM compares favorably to diverse baseline classifiers and regression methods, paying particular attention to how SPSM improves sample efficiency in learning over non-sharing pattern submodels (Section 5).

2 Prediction with test-time missingness

Let $X = [X_1, \dots, X_d]^\top$ be a vector of d random variables taking values in $\mathcal{X} \subseteq \mathbb{R}^d$, and $M = [M_1, \dots, M_d]^\top$ be a random missingness mask in $\mathcal{M} \subseteq \{0, 1\}^d$ where $M_j = 1$ indicates that variable X_j is missing. Next, let $\tilde{X} \in (\mathbb{R} \cup \{\text{NA}\})^d$ be the mixed observed-and-missing values of X according to M and define $X_{-M} = [X_j : M_j = 0]^\top \in \mathbb{R}^{d - \|M\|_1}$ to be the vector of *observed* covariates under M . The outcome of interest, $Y \in \mathbb{R}$, may depend on all of X , observed or missing, as well as on M . Let $k = |\mathcal{M}|$ denote the number of possible missingness patterns.¹ Further, assume that variables X, M, Y are distributed according to a *fixed, unknown* joint distribution p .

¹In practical scenarios, we expect k to be much smaller than the worst-case number, 2^d .

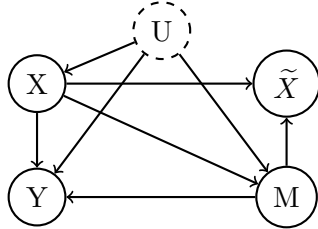


Figure 2: Directed graph showing assumed probabilistic dependencies. \tilde{X} is a deterministic function of X, M . Unobserved variables U may influence both covariates X , missingness M and the outcome Y , ruling out “missing at random” (MAR).

Figure 2 illustrates the assumed causal dependencies of the variables used, coinciding most closely with *selection missingness* (Little, 1993). The graph literature states, when X_{-M} , the partially observed variable and the missingness mask M both point to another variable, the outcome Y , the corresponding conditional distribution is not identifiable non-parametrically (Bhattacharya et al., 2020).

Our goal is to predict Y under missingness M in X using functions $f : (\mathbb{R} \cup \{\text{NA}\})^d \rightarrow \mathbb{R}$. We aim to minimize risk with respect to the squared loss on p ,

$$\min_f R(f), \text{ where } R(f) := \mathbb{E}_{\tilde{X}, Y \sim p}[(f(\tilde{X}) - Y)^2]. \quad (1)$$

Under the assumption that Y has centered, additive noise,

$$Y = g(X, M) + \epsilon \text{ where } \mathbb{E}[\epsilon] = 0, \quad (2)$$

the Bayes-optimal predictor of Y is the function

$$f^* = \mathbb{E}[Y \mid X_{-M}, M]$$

In general, observed values X_{-M} are insufficient for predicting Y ; f^* depends directly on the mask M (Le Morvan et al., 2021), *even if Y does not depend directly on M* .

A common strategy to learn f is to first impute the missing values in \tilde{X} and then fit a model on the observed-or-imputed covariates $X^I \in \mathbb{R}$ —so-called *impute-then-regress* estimation. Even though imputation is powerful, it is not always optimal under test-time missingness (Le Morvan et al., 2021) and often assumes that data is missing at random (MAR) (Carpenter and Kenward, 2012; Seaman et al., 2013).

2.1 Pattern submodels

In cases where the number of distinct patterns k is small, it is possible to learn separate predictors f_m for each missingness pattern. This idea has been called *pattern submodels* (PSM) (Fletcher Mercaldo and Blume, 2020; Marshall et al., 2002). In their basic form, PSM aim to minimize the empirical risk under each missingness pattern.

Let $D = \{(\tilde{x}^{(1)}, m^{(1)}, y^{(1)}), \dots, (\tilde{x}^{(n)}, m^{(n)}, y^{(n)})\}$ be a data set of n samples, with partially observed features $\tilde{x}^{(i)}$, corresponding to missingness patterns $m^{(i)}$, drawn independently and identically distributed from p . PSM may be learned by minimizing the regularized empirical risk,

$$\min_{\{f_m\} \in \mathcal{F}^k} \frac{1}{n} \sum_{i=1}^n L(f_{m^{(i)}}(\tilde{x}^{(i)}), y^{(i)}) + \sum_{m \in \mathcal{M}} \mathcal{R}(f_m) \quad (3)$$

over a suitable class of models \mathcal{F} and regularization \mathcal{R} . Fletcher Mercaldo and Blume (2020) considered linear and logistic regression models, $f_m = \sigma(\theta_m^\top x)$ with σ either the identity or logistic function and loss L chosen to match.

The objective in (3) is separable in m and can be solved independently for each pattern. However, this often leads to high variance in the small-sample regime since each pattern accounts for only a subset of the available samples. Without structural assumptions, the number of patterns k grow exponentially with d . To combat variance, (Fletcher Mercaldo and Blume, 2020) required a sample size of at least $2d$ per pattern, to fit a pattern-specific model, reverting to a so-called *complete-case model* for less frequent patterns. Bertsimas et al. (2021) took a different approach, fitting submodels to clusters of patterns found using a greedy, divisive algorithm. We describe this more in Section 6.

PSM allow for prediction under test-time missingness which adapts to the pattern m without relying on imputation or assumptions on missingness mechanisms like MAR. However, the prediction target (and the Bayes-optimal model f^*) may have only a small dependence on the pattern m ; *the optimal submodels for all m may share significant structure*. Next, we propose estimators that exploit such structure to reduce variance and increase interpretability.

3 Sharing pattern submodels

There are many scenarios where test-time predictions are made based on inputs with missing values, and the missingness often has informative structure. In this section, we present *sharing pattern submodels* as a possible solution and begin by giving a motivating example.

Running example: Alzheimer’s disease progression Consider a situation where physicians at different memory clinics want to predict the progression of dementia, e.g., Alzheimer’s disease, in a subject (see Figure 1). Which data are collected at each site depends on the availability of measurement tools and the health status of the patients. For example, only a subset of clinics may be equipped to do blood work or genetic testing. Assume for simplicity that the pattern of missing values is unique to each clinic. In this way, a pattern-specific model is also site-specific. Fitting a separate model for each clinic may be difficult if each clinic has a relatively small patient population, and does not make efficient use of data collected at other clinics (high variance); in many cases, we expect the mechanisms which relate inputs to outcomes to be shared. Conversely, using a single model for all clinics may be suboptimal for all of them if the clinics see different patients, make different measurements, or treat patients differently (high bias). Therefore, sharing relevant information between clinics to learn *similar* models while allowing each clinic to specialize their models somewhat can lead to a favorable tradeoff of bias and variance. In addition, the simpler any differences between models can be described, the easier for domain experts to compare how predictions would differ between clinics, leading to increased interpretability.

3.1 Sharing Pattern Submodels

We propose sharing information between submodels, specific to missingness patterns, by imposing similarity regularization to the objective in (3) and solving the resulting coupled optimization. We apply this idea to linear and logistic regression next. In general, these models need not be well-specified—we do not make assumptions on the functional form of Y or the distribution of the noise ϵ . In many applications, linear models are found to be useful approximations of nonlinear functions. In Section 4, we analyze the case where the data generating process is linear as well.

Let $\theta \in \mathbb{R}^d$ represent *main model* coefficients used in prediction under all missingness patterns, and define $\theta_{-m} = [\theta_j : m_j = 0]^\top \in \mathbb{R}^{d_m}$ to be the subset of coefficients

corresponding to variables observed under m . To emphasize, $\theta_{\neg m}$ depends only on m in selecting a subset of θ . Similarly, define $\Delta_{\neg m} \in \mathbb{R}^{d_m}$ to be *pattern-specific specialization* of these coefficients to m . In contrast to θ , $\Delta_{\neg m}$ is unique to each pattern m . In regression tasks, we aim to learn pattern submodels on the form

$$f_m(x) := (\theta_{\neg m} + \Delta_{\neg m})^\top x_{\neg m} \quad (4)$$

by solving the following problem with $\lambda_m \geq 0$ and $\gamma \geq 0$,

$$\begin{aligned} \underset{\theta, \{\Delta_{\neg m}\}}{\text{minimize}} \quad & \frac{1}{n} \sum_{i=1}^n ((\theta_{\neg m^{(i)}} + \Delta_{\neg m^{(i)}})^\top x_{\neg m^{(i)}} - y^{(i)})^2 \\ & + \frac{\gamma}{n} \|\theta\| + \sum_{m \in \mathcal{M}} \frac{\lambda_m}{n_m} \|\Delta_{\neg m}\|_1 . \end{aligned} \quad (5)$$

where n_m is the number of samples of pattern m . Intercepts (bias terms) are left out for brevity. We call the solution to (5) sharing pattern submodels (SPSM). In classification tasks, the square loss is replaced by the logistic loss. The optimization problem is convex, and we find optimal values for θ and Δ_m using L-BFGS-B (Byrd et al., 1995) in experiments.

λ_m and γ in (5) are regularization parameters. For the term $\|\theta\|$, we use either the ℓ_1 or ℓ_2 norm to tradeoff bias and variance in the main model. A high value for λ_m regularizes the adaptation of model coefficients to missingness pattern m such that high λ_m encourages smaller $\|\Delta_m\|_1$ and greater coefficient sharing. In experiments, we let λ_m take the same value for all patterns. ℓ_1 -regularization is used for Δ as we aim for a sparse solution where the majority of adaptation coefficients are zero.

Why is SPSM more interpretable? Sparsity is a generally useful measure of interpretability (Rudin, 2019), since it results in only a subset of the input features affecting predictions, reducing the effective complexity of the model (Miller, 1956; Cowan, 2010). In our setting, we focus on sparsity in *specializations* of pattern coefficients, Δ_m , and argue that a set of submodels is more interpretable if they contain fewer non-zero coefficients, $\sum_m \|\Delta_m\|_0$ is small. Comparing pattern specializations allows domain experts to reason about how similar submodels are, and how they are affected by missing values. In the context of Alzheimer’s progression, predictions without certain biomarkers may have to rely more strongly on a small number of related variables, but the coefficients of unrelated variables may be unaffected.

4 Optimality and sparsity

Objective (5) is used to learn submodels on the form $(\theta_{\neg m} + \Delta_{\neg m})^\top X_{\neg m}$ where θ is shared between patterns and $\Delta_{\neg m}$ is sparse. While this will lead to lower variance (Tibshirani, 1996) and greater interpretability, it may introduce bias. When is this trade-off beneficial? Surprisingly, in this section, we prove that there exist DGPs where a sparse model with the form of SPSM is optimal—even when the true outcome depends on partially unobserved components of X and on M itself—and describe the conditions which need to hold for bias to be small or zero.

A model with no pattern specialization (complete sparsity) is trivially optimal if the outcome of interest Y depends *only* on features in $X_{\neg M}$, observed under M . However, this assumption is often unrealistic in practice. To emphasise this point, let us return to the motivating example in Section 3. When predicting Alzheimer’s disease progression based on measured health data, we do not expect *access* to equipment for genetic testing to have an impact on whether genetic factors influence disease progression. However, whether this equipment is *used*, if available, may depend on a patient’s condition.

A less restrictive setting is where Y depends linearly on all components of X , and on the pattern M , but not on interactions between X and M ,

$$Y = \theta^\top X + \alpha_m + \epsilon, \text{ with } \mathbb{E}[\epsilon] = 0, \quad (6)$$

where α_m is a pattern-specific intercept. Without α_m , this is a setting often targeted by imputation methods, since the outcome is a parametric function of the full X . However, we know that X will be partially missing also at test time. Next, we study this setting with Gaussian X , where we can precisely characterize the optimal model and its sparsity.

4.1 Sharing in linear-Gaussian settings

Recall that $X_{\neg m}$ and $\theta_{\neg m}$ denote covariates and coefficients corresponding to *observed* variables under pattern m , respectively, and define X_m and θ_m analogously for missing variables. Then, under (6), the Bayes-optimal model is

$$\begin{aligned} \mathbb{E}[Y \mid X_{\neg m}, M = m] &= \theta_{\neg m}^\top X_{\neg m} + \mathbb{E}_{X_m}[\theta_m^\top X_m + \alpha_m \mid X_{\neg m}, M = m] \\ &= \theta_{\neg m}^\top X_{\neg m} + \xi_m \end{aligned} \quad (7)$$

with $\xi_m = \theta_m^\top \mathbb{E}_{X_m}[X_m \mid X_{\neg m}] + \alpha_m$ the bias of the naïve prediction made using only the coefficients $\theta_{\neg m}$ of the main model corresponding to observed features. Ignoring ξ_m coincides with performing prediction following zero-imputation and is suboptimal in general when ξ_m is dependent on $X_{\neg m}$.

Assume that covariates X_1, \dots, X_d are distributed according to a multivariate Normal distribution, $X \sim \mathcal{N}(\mu, \Sigma)$ with mean μ and covariance matrix Σ . We make this assumption only for the theoretical analysis in this section. Further, let $\Sigma_{\neg m, m}$ denote the submatrix of Σ restricted to the rows corresponding to *observed* variables under m and columns corresponding to those *missing* under m , and define $\Sigma_{\neg m, \neg m}$ and $\Sigma_{m, \neg m}$ analogously.

Example 1. Under the conditions above (Normal X , outcome as in (6)), the Bayes-optimal predictor for an arbitrary missingness mask $m \in \mathcal{M}$, is

$$f_m^* = \mathbb{E}[Y \mid X_{\neg m}, m] = (\theta_{\neg m} + \Delta_{\neg m}^*)^\top X_{\neg m} + C_m$$

where $C_m \in \mathbb{R}$ is constant with respect to $X_{\neg m}$ and

$$\Delta_{\neg m}^* = (\Sigma_{\neg m, \neg m}^{-1})^\top \Sigma_{\neg m, m} \theta_m.$$

The result is proven in Appendix A. In words, Example 1 states that, for a linear-Gaussian system, the Bayes-optimal model under missingness pattern m has the form of SPSM with pattern-specific intercept, combining coefficients of a shared model θ and specializations $\Delta_{\neg m}^*$. Unfortunately, this is not the case in general: there exists an optimal correction term $\Delta_{\neg m}^*$ which is constant with respect to $X_{\neg m}$ if and only if X, M, Y obey the conditions of Example 1. The result follows directly from (7), in which the last step can be performed only in the linear-Gaussian setting. Despite this, SPSM may achieve a better bias-variance tradeoff than other estimators; the result only means that the Bayes-optimal model is not always linear. Indeed, we find on real-world data that SPSM is often preferable to strong nonlinear baselines.

Is it possible to recover the true θ for SPSM? Like other regularized linear estimators, e.g., Ridge, LASSO, SPSM is biased for finite samples. In the infinite-sample limit, SPSM recovers the true θ in the same way as the methods mentioned above:

Table 1: Extreme cases and equivalences of SPSM, provided that no pattern-specific intercept is used.

	$\gamma < \infty$	$\gamma = \infty$
$\lambda_m = \infty$	Zero imputation	Constant
$0 < \lambda_m < \infty$	Partial sharing	Pattern submodel
$\lambda_m = 0$	No sharing	Pattern submodel

the regularization terms vanish due to the normalization with n , and the sum of the minimizers $(\theta + \Delta_{\neg M})$ of the SPSM objective (5) coincide with (unregulated) OLS estimates $(\theta_{\neg M})$, which are independently fitted for each missingness pattern k . Individual parameters θ and $\Delta_{\neg M}$ are identified only up to addition in the unregularized case. Due to the consistency of OLS, we have the same guarantee. We do not yet have finite-sample guarantees for recovery of the sparsity pattern in Δ . However note, that 'true' sparsity in Δ need not exist even if the true θ is shared between all patterns and is sparse—it relies also on the dependence between covariates.

When is the optimal pattern specialization sparse?

Assume that the conditions of Example 1 hold. We characterize below cases in which the optimal model $(\theta^*, \{\Delta_{\neg m}^*\})$ is sparse in Δ , justifying the regularization used in SPSM. For the optimal specialization $\Delta_{\neg m}^*$ to be sparse in coefficient j , i.e., $\Delta_{\neg m}^*(j) = 0$, it must be that $\Sigma_{\neg m(j), m} = \mathbf{0}$ or that $\Sigma_{\neg m(j), m} \theta_m = \mathbf{0}$.

In linear-Gaussian systems, we identify the following cases when we can expect a model for missingness pattern m that is sparse in $\Delta_{\neg m}$ to have small bias with respect to $\Delta_{\neg m}^*$:

1. Unobserved variables are not predictive, $\theta_m \approx 0$.
2. Observed and unobserved variables under m are uncorrelated, $\Sigma_{m, \neg m} \approx 0$.
3. Unobserved variables which are correlated with observed variables are not predictive, $\Sigma_{\neg m, m} \theta_m \approx 0$.

Conversely, specialization, i.e., $\Delta_{\neg m}^*(j) \neq 0$, is *needed for features j that are predictive and redundant (replicated well by unobserved features which are also predictive)*. This is because in the main model, redundant variables may share the predictive burden, but when they are partitioned by missingness, they have to carry it alone. This shows that prediction with a single model and zero-imputation is sub-optimal in general.

4.2 Relationship to other methods

For particular extreme values of the regularization parameters γ, λ_m , SPSM coincides with other methods; see Table 1. First, the full-sharing model ($\lambda_m = \infty, \gamma < \infty$) coincides with fitting a single model to all samples after zero-imputation. To see this, set $\Delta_m = 0$ for all m and note

$$\theta_{\neg m^{(i)}}^\top x_{\neg m^{(i)}}^{(i)} = \theta^\top I_0(\tilde{x}^{(i)})$$

where $I_0(\tilde{x})$ replaces missing values in \tilde{x} with 0. In this setting, submodel coefficients cannot adapt to m . In implementation we allow the fitting of pattern-specific intercepts which are not regularized by λ_m .

Second, $(\lambda_m < \infty, \gamma = \infty)$ coincides with the standard pattern submodel without parameter sharing (Fletcher Mercaldo and Blume, 2020) or the ExtendedLR method

of (Morvan et al., 2020). The precise nature of this equivalence depends on the choice of regularization.² In this setting, each submodel \hat{f}_m is fit completely independently of every other, and is therefore sensitive to variance.

Finally, an **SPSM** model with optimal parameters θ and $\Delta_{\neg m}^*$ in the linear-Gaussian case, implicitly makes a perfect single linear imputation,

$$\mathbb{E}[X_m | X_{\neg m}] = X_{\neg m}(\Sigma_{\neg m, \neg m}^{-1})^\top \Sigma_{\neg m, m},$$

and applies the main model’s parameters θ_m to the imputed values. If many samples are available, it may be feasible to learn Σ directly. In this case, impute-then-regress is also optimal in expectation. However, if the variables in $X_{\neg m}$ and X_m are never observed together, imputation is no longer possible. In contrast, **SPSM** could still learn an optimal submodel for each pattern, given enough samples.

5 Experiments

We evaluate the proposed **SPSM** model³ on simulated data and on two publicly available datasets, aiming to answer two main questions: How does the accuracy of **SPSM** compare to baseline models, including impute-then-regress, for small and larger samples; How does sparsity in pattern specializations Δ affect performance and interpretation? In choosing baselines, it was important for us to compare with standard procedures (imputation, XGBoost) used when applied to clinical problems. Particular focus was placed on the evaluation of sampling efficiency and interpretability.

Experimental setup

In the first step of the **SPSM** algorithm, performed before one-hot-encoding of categorical features, all missingness patterns in the training set are identified. In all subsequent steps, only missingness patterns from the training set are used.

Both linear and logistic variants of **SPSM** were trained using the L-BFGS-B solver provided as part of the SciPy Python package (Virtanen et al., 2020). Our implementation supports both ℓ_1 and ℓ_2 -regularization of the main model parameters θ and ℓ_1 -regularization of pattern-specific deviations Δ . This includes both the no-sharing pattern submodel ($\lambda_m < \infty, \gamma = \infty$) and full-sharing model ($\lambda_m = \infty, \gamma < \infty$) as special cases. In the experiments, γ can take values within $[0, 0.1, 1, 5, 10, 100]$, and we used a shared $\lambda_m = \lambda \in [1, 5, 10, 100, 1000, 1e8]$ for all patterns. Intercepts were added for both the main model and for each pattern without regularization. We do not require patterns to have a minimum sample size but support this functionality. For missingness patterns at test time that did not occur in the training data, variables were removed until the closest training pattern was recovered.

We compare to the following baseline methods:

Imputation + Ridge / logistic regression (Ridge/LR) the data is first imputed (see below) and a ridge or logistic regression is fit on the imputed data.

Imputation + Multilayer perceptron (MLP): The MLP estimator is based on a single hidden layer of size $\in [10, 20, 30]$ followed by a ReLu activation function and a softmax layer for classification tasks and a linear layer for regressions tasks. As input, the imputed data concatenated with the missingness mask. The MLP is trained using ADAM (Kingma and Ba, 2014), and the learning rate is initialized to constant (0.001) or adaptive. We use the implementation in SciKit-Learn (Pedregosa et al., 2011).

²Fletcher Mercaldo and Blume (2020) adopted a two-stage estimation procedure, the relaxed LASSO (Meinshausen, 2007).

³Code to reproduce experiments will be made available upon de-anonymization of this work.

Pattern submodel (PSM): For each pattern of missing data, a linear or logistic regression model is fitted, separately regularized with a ℓ_2 penalty. Following Fletcher Mercaldo and Blume (2020), for patterns with fewer than $2 * d$ samples available, a complete-case model (CC) is used. Our implementation of PSM is based on a special case of our **SPSM** implementation where regularization is applied over all patterns and not in each pattern separately. To enforce fitting separated submodels for each pattern, we set $\gamma = 1e^8$ and $\lambda = 0$.

XGBoost (XGB): XGBoost is an implementation of gradient boosted decision trees. Note, XGBoost supports missing values by default (Chen et al., 2019), where branch directions for missing values are learned during training. A logistic classifier is then fit using XGBClassifier while regression tasks are trained with the XGBRegressor (Pedregosa et al., 2011). We set the hyperparameters to 100 for the number of estimators used, and fix the learning rate to 1.0. The maximal depth of the trees is $\in [5, 10, 15]$.

For imputation, we either use zero imputation (I_0), mean imputation (I_μ) or iterative imputation (I_{it}), as implemented using the IterativeImputer in SciKit-Learn (Pedregosa et al., 2011; Van Buuren, 2018). XGB’s handling of missing values is denoted I_n . Imputation methods and hyperparameters for all methods were selected based on the validation portion of random 64/16/20 training/validation/test splits. Results were averaged over five random splits of the data set. The performance metrics for classification tasks were accuracy and the Area Under the ROC Curve (AUC). For regression tasks we use the mean squared error (MSE) and the general coefficient of determination, the R-square, (R^2) value, taking values in $[-\infty, 1]$ where negative values represent predictions worse than the mean (Dancer and Tremayne, 2005). Confidence intervals at significance level $\alpha = 0.05$ are computed based on the number of test set samples. For accuracy, MSE and R^2 we use a Binomial proportion confidence interval (Fagerland et al., 2015) and for AUC we use the classical model of (Hanley and McNeil, 1983).

5.1 Simulated data

We use simulated data to illustrate the behavior of sharing pattern submodels and baselines in the context of Example 1, focusing on the bias and variance of the various methods. To do this, we sample d input features X from a multivariate normal $\mathcal{N}(0, \Sigma)$ with covariance matrix Σ specified by a cluster structure; the features are partitioned into k clusters of equal size. The covariance is defined as $\Sigma_{ii} = 1$, $\Sigma_{i \neq j} = 0$ if i, j are in different clusters, and $\Sigma_{i \neq j} = c$ if i, j are in the same cluster, where c is chosen as large as possible so that Σ remains positive semidefinite. Each cluster $c \in \{1, \dots, k\}$ is represented in the outcome function $Y = \beta^\top X + \epsilon$ by a single feature $i(c)$, such that $\beta_{i(c)} \sim \mathcal{N}(0, 1)$ and $\beta_j = 0$ for other features. We let $\epsilon \sim \mathcal{N}(0, 1)$, independently for each sample. We consider two missingness settings: In Setting A, each variable in cluster c is missing if $X_{i(c)} > -0.5$. In Setting B, each variable in cluster c —except one chosen uniformly at random—is missing if $X_{i(c)} > -0.5$. Here, we generate samples with $d = 20$ and $k = 5$. Both settings satisfy the conditions of Example 1.

In Figure 3, we see the test-set R^2 for Setting A for **SPSM** and baselines. We note that methods using zero imputation (imputation method selected based on validation error at each dataset size) perform well initially but plateau quickly, indicating relatively high bias. **SPSM** and **PSM** both achieve a higher R^2 for the full sample. **SPSM** performs better than **PSM** for small samples indicating lower variance. The **SPSM** model includes 42 non-zero pattern-specific coefficients when the dataset fraction is 0.2 and 68 with the fraction is 0.8. Results for Setting B are similar and presented in the Appendix.

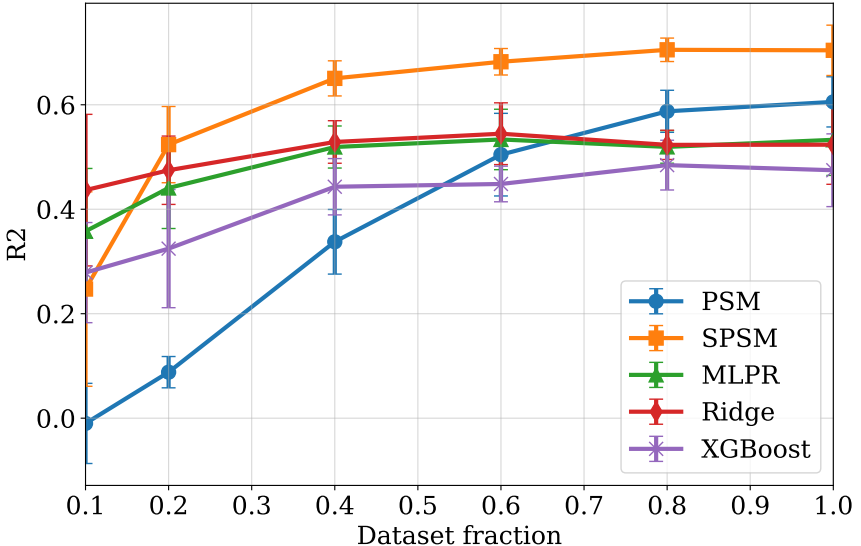


Figure 3: Performance on simulated data Setting A. Error bars indicate standard deviation over 5 random data splits. The complete dataset has $n = 2000$ samples. Zero imputation was used for MLP, Ridge and XGB.

5.2 Real-world tasks

We describe two health care data sets used for both classification and regression tasks below.

ADNI The data is obtained from the publicly available Alzheimer’s Disease Neuroimaging Initiative (ADNI) database.⁴ ADNI collects clinical data, neuroimaging and genetic data, biological markers, and clinical and neuropsychological assessments from study subjects. The compiled data set includes 1337 subjects that were preprocessed by one-hot encoding of the categorical features and standardized for the numeric features. The processed data has 37 features and 20 unique missingness patterns. In the classification task, we predict if a patient’s diagnosis will change 2 years after baseline diagnosis. The label set is quite unbalance showing 1089 patients who do not change from their baseline diagnosis, and 248 do. The regression task targets predicting the result of the cognitive test ADAS13 (Alzheimer’s Disease Assessment Scale) at a 2 year follow-up (Mofrad et al., 2021) based on available data at baseline.

SUPPORT The second task is based on the Study to Understand Prognoses and Preferences for Outcomes and Risks of Treatments (SUPPORT) (Knaus et al., 1995). The primary goal of the study was to model survival over a 180-day period in seriously ill hospitalized adults. A component of the SUPPORT prognostic model was the SUPPORT day 3 Physiology Score (SPS), a risk score created to account for various sources of health variation and co-morbidities, with range [0, 100]. The following 10 covariates were selected and standardized: partial pressure of oxygen in the arterial blood (pafi), mean blood pressure, white blood count, albumin, APACHE III respiration score, temperature, heart rate per minute, bilirubin, creatinine, and sodium. The data set contains 9104 subjects represented by 23 unique missingness pattern. Following Fletcher Mercaldo and Blume (2020), in the regression task we predict the SPS while for the classification task, we predict if a patient’s SPS is above the median; the label rate is 50/50 by definition. We mimic their MNAR setting by adding 25 units to the SPS values of subjects missing the covariate pafi.

⁴<http://adni.loni.usc.edu>

Table 2: Results for ADNI and SUPPORT tasks along with the respective imputation method (see setup). We also report the number of non-zero coefficients in shared (k) and pattern-specific models (l) as $k + l$.

Regression	R^2	# Coefficients
ADNI		
Ridge, I_μ	0.66 (0.59, 0.73)	37 + 0
XGB, I_μ	0.41 (0.31, 0.50)	—
MLP, I_0	0.62 (0.55, 0.69)	—
PSM	0.51 (0.43, 0.60)	0 + 430
SPSM	0.66 (0.59, 0.73)	37 + 21
SUPPORT		
Ridge, I_0	0.38 (0.35, 0.42)	11 + 0
XGB, I_n	0.30 (0.27, 0.34)	—
MLP, I_μ	0.56 (0.53, 0.59)	—
PSM	0.52 (0.49, 0.56)	0 + 188
SPSM	0.53 (0.50, 0.56)	11 + 91
Classification	AUC	Accuracy
ADNI		
LR, I_0	0.85 (0.80, 0.90)	0.85 (0.74, 0.94)
XGB, I_n	0.80 (0.74, 0.86)	0.84 (0.73, 0.94)
MLP, I_0	0.86 (0.78, 0.89)	0.84 (0.73, 0.94)
PSM	0.81 (0.75, 0.87)	0.84 (0.74, 0.95)
SPSM	0.86 (0.81, 0.90)	0.85 (0.75, 0.96)
SUPPORT		
LR, I_0	0.83 (0.81, 0.85)	0.77 (0.74, 0.79)
XGB, I_0	0.85 (0.83, 0.87)	0.78 (0.75, 0.81)
MLP, I_0	0.86 (0.85, 0.88)	0.79 (0.76, 0.81)
PSM	0.84 (0.83, 0.86)	0.78 (0.75, 0.81)
SPSM	0.85 (0.83, 0.86)	0.78 (0.75, 0.80)

5.3 Results

We report the results on the two health data sets in Table 2. For regression models, we provide the number of non-zero coefficients used by the linear models. In addition, we study prediction performance as a function of data set size in Figure 4 and in supplementary Figure 6. The statistical uncertainty of the average error or average performance is expressed through confidence intervals. The results of the HOUSING data set are presented in the appendix B.3 as an example of a non-healthcare related data set.

For ADNI regression, SPSM and Ridge are the best performing models with a R^2 score of 0.66 showing the same confidence in the prediction. Validation performance resulted in $\gamma = 10.0$, $\lambda = 50$ for SPSM. With an R^2 score of 0.51, PSM seems not able to benefit from pattern-specificity in the data set. In contrast, SPSM benefits from coefficient sharing which results in a significant smaller number of coefficients compared to PSM. For SUPPORT regression, PSM achieved almost the same result as SPSM (R^2 score of 0.52–0.53) with partly overlapping confidence intervals for the predictions. Although, the number of coefficients used in SPSM is smaller than in PSM due to the coefficient sharing between submodels. The best values for $\gamma = 0.1$ and $\lambda = 5.0$ are lower than for ADNI, which is consistent with the larger data set

size. The best performing model is the **MLP**, with an R^2 value of 0.56, however, the black-box nature of **MLP** is not conducive to reasoning about the influence of the missingness pattern. Across both data sets, mean and zero imputation had the best validation performance for **Ridge**, **XGB** and **MLP**. In summary, **SPSM** was consistently among the best performing models in both data sets, with comparatively tight confidence intervals.

In classification, we see that for **ADNI**, **SPSM**, **MLP** and **LR** achieve the highest prediction accuracy (0.84–0.85) and AUC (0.85–0.86). All methods perform similarly well on **ADNI**. **SPSM** selected $\gamma = 0$ and sharing regularisation of $\lambda = 1.0$ which indicates moderate coefficient sharing. For the **SUPPORT** data, all models perform almost at the same level. **XGB** and **MLP** perform slightly better than **SPSM**. **PSM** and **SPSM** achieve very comparable results. The **SPSM** model has a γ value of 0.1 and $\lambda = 10.0$. Across **ADNI** and **SUPPORT** **LR**, **XGB** and **MLP** predominantly use zero imputation and. In all tasks, **SPSM** compares comparably or favorably to all other methods. The tight confidence intervals for the classification tasks in both data sets indicate high certainty in the result averages.

Non-healthcare data set and coefficients specialization In contrast to the previous two data sets, where sharing coefficients is beneficial, for the **HOUSING** data set, we see a large benefit from nonlinear estimation: the tree-based approach **XGB**, showing an R^2 of 0.76 outperforms the other approaches for the regression task confirms the non-linearity of that data set. We also do not see the same positive effect in specializing (**PSM**, **SPSM** not better than **Ridge** with imputation). None of the missing value indicators show a significant feature importance level in **XGB** which might also indicate that pattern specialization is not necessary for the **HOUSING** data set. For more detailed results on the **HOUSING** data set see appendix B.3.

Performance with varying training set size In Figure 4, we show the test R^2 for linear models trained on different fractions of the **ADNI**. Each set was subsampled into fractions 0.2, 0.4, 0.6, 0.8, 1.0 of the full data sets, respectively. On **ADNI**, especially for small fractions, **SPSM** benefits from coefficient sharing and lower variance data compared to **PSM**. **Ridge** with mean imputation performs comparably here. A similar figure for the **SUPPORT** data is presented in the supplementary Figure 6. **SPSM** and **PSM** perform equally well across the fractions, whereas **Ridge** shows high error compared to both pattern submodels.

Pattern specialization in **SPSM**

We inspect pattern specializations Δ for **SPSM** in the **ADNI** regression task. In Table 3, we present the main model θ and pattern-specific coefficients Δ_4 for pattern 4. Table 7 in the appendix shows all patterns with $\Delta \neq 0$.

For pattern 4, measurements of amyloid- β peptides and TAU and PTAU, two proteins measured in the brain, are missing from the baseline diagnostics (Alzheimer’s Disease Neuroimaging Initiative, 2012). The absence of these three features affects pattern specialization: For FDG-PET (fluorodeoxyglucose), an imaging test used to detect lymphoma and other cancers, the magnitude of its coefficient is increased, placing heavier weight on the feature in prediction. Similarly, the coefficients for fusiform, the brain area for object and face recognition, and intracranial volume (ICV) increase in magnitude and predictive significance when ABETA, TAU, and PTAU are absent (Alzheimer’s Disease Neuroimaging Initiative, 2012). In contrast, for the feature ”age,” the resulting coefficient of -0.019 (compared to 0.121 in the main model) means that the predictive influence of this feature decreases under pattern 4.

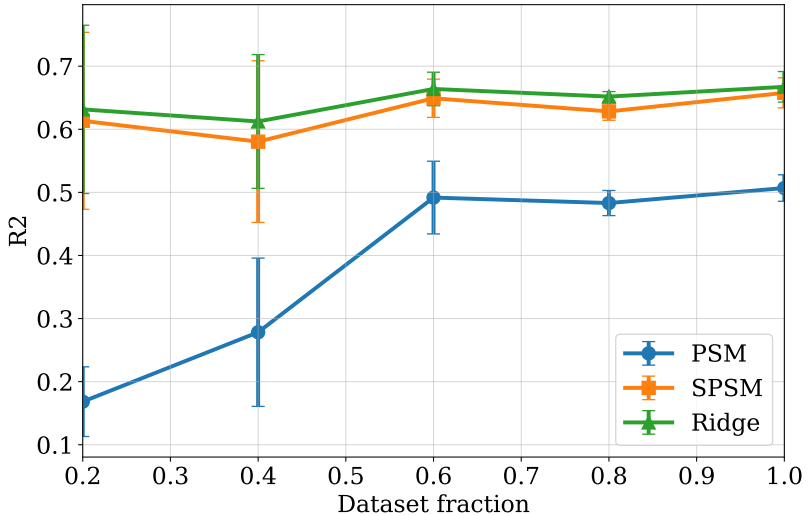


Figure 4: Performance on ADNI data for the regression task. Error bars indicate standard deviation over 5 random subsamples of the data. Equal performance for SPSM and Ridge and subpar performance for PSM indicates that for ADNI regression, pattern specialization is mostly irrelevant.

As Table 3 shows, SPSM applied to tabular data allows for short descriptions of pattern specialization, which helps construct a simple and meaningful model. We enforce sparsity in Δ to limit the number of differences between submodels, and present all features j with specialized coefficients $\Delta_{-m}(j) \neq 0$, five in the example case. In this way, the set of submodels is more interpretable and the viewer, e.g. medical staff can be supported in decision making.

Trade-off between interpretability and accuracy The interpretability-accuracy trade-off is especially crucial for practical use of our model. The empirical results do not show any significant evidence that our proposed sparsity regularization hurts prediction accuracy (see e.g., Table 2, Figure 4). Nevertheless, in a practical scenario, domain experts may have to choose a simpler model at a slight cost in performance. In such a setting, we can measure the trade-off by varying values of hyperparameters to find an adequate balance (see Figure 7 in the Appendix using an example of the SUPPORT data). The parameter selection is based on the validation set and aligns with the test set results. We see some parameter sensitivity that supports sharing but only in a moderate way.

6 Related work

Pattern-mixture missingness refers to distributions well-described by an independent missingness component and a covariate model dependent on this pattern (Rubin, 1976; Little, 1993; Little and Rubin, 1986). Here, *pattern missingness* refers to emergent patterns which may or may not depend on observed covariates, consistent with Marshall et al. (2002). As described previously, Fletcher Mercaldo and Blume (2020); Morvan et al. (2020) and Bertsimas et al. (2021) used this setting to define pattern submodels for flexible handling of missingness at test time. Note, for example, the ExtendedLR method of (Morvan et al., 2020) represents a related method to pattern submodels, however, they neither study coefficient sharing between models nor provide a theoretical analysis of when optimal submodels have partly identical coefficients (sharing, sparsity in specialization). Recognizing the variance problems

Table 3: Example of Δ_4 in the regression task using SPSM using ADNI. The SPSM takes $\gamma = 10$ and $\lambda = 13$ as parameters for a single seed. There are 10 missingness pattern in total, while 4 of them have non-zero coefficients for Δ . Coefficients are for standardized variables.

Missing features in pattern 4:			
ABETA, TAU and PTAU at baseline (bl)			
Feature	Δ_4	θ	$\theta + \Delta_4$
Age	-0.140	0.121	-0.019
FDG-PET	-0.090	-0.039	-0.129
Whole Brain (bl)	0.000	-0.045	-0.044
Fusiform	0.016	0.021	0.037
ICV	0.001	0.093	0.094
Intercept	-0.10	0.18	

involved, Marshall et al. (2002) described the one-step sweep (OSS) method using estimated coefficients and augmented covariance matrix obtained from fully observed data for predictions for individuals with incomplete information at test time.

In very recent and so far unpublished work, Bertsimas et al. (2021) presents two related methods for predicting with missingness at test time. First, *affinely adaptive regression* specializes a shared model by applying a coefficient correction given by a linear function of the missingness pattern m . When the number of variables d is smaller than the number of patterns (which could grow as 2^d), this greatly restricts the number of possible specializations. It is possible that their regularization would result in a different bias-variance tradeoff than our method, but unlike our work, it is not justified by theoretical analysis. Second, *finitely adaptive regression* starts by placing each pattern in the same model, recursively partitioning them into subsets.

Several methods based on deep learning have been proposed which are applicable for prediction under test-time missingness with or without explicitly attempting to impute missing values (Bengio and Gingras, 1995; Tresp and Briegel, 1997; Che et al., 2018; Le Morvan et al., 2020; Morvan et al., 2020). For example, the NeuMiss networks propose a new type of non-linearity: the multiplication by the missingness indicator (Le Morvan et al., 2020). Che et al. (2018) aims to exploit the missing patterns for effective imputation in multivariate time series prediction. They use recurrent neural networks that take two representations of missing patterns, i.e., masking and time interval, and incorporate them into a deep model architecture. Nazabal et al. (2020) uses a generative model that handles mixed numerical and nominal likelihood models parameterized with deep neural networks to design variational autoencoders suitable for fitting incomplete heterogeneous data. However, neither of these approaches aim to take advantage of recurring missingness patterns.

7 Discussion and Conclusion

We have presented sharing pattern submodels (SPSM) for prediction with missing values. The method exploits recurring pattern structure in missingness, fitting a shared model for different patterns while allowing limited pattern-specific specialization. We have described settings where sharing is provably optimal even when the prediction target depends on both missing values and on the missingness pattern itself. Experimental results, based on real-world and synthetic data, confirm that SPSM performs the classification and regression tasks comparably or slightly better than diverse baseline models across all data sets, while being independent of imputation and allowing effective use of the available data across patterns. Notably,

the proposed method never performs worse than non-sharing pattern submodels as these do not use the available data efficiently.

By enforcing sparsity in pattern specialization, we ensure that the resulting subset of features is reduced to relevant differences which will foster interpretability for domain experts; **SPSM** allows for more straight-forward reasoning about the similarity between submodels and the effects of missingness. Lipton et al. (2016) provides qualitative design criteria to address model properties and techniques thought to confer interpretability. We will show that **SPSM** satisfies some form of transparency by asking, i.e., *how does the model work?*. As stated in (Lipton et al., 2016), transparency is the absence of opacity or black-boxness meaning that the mechanism by which the model works is understood by a human in some way. We evaluate transparency at the level of the entire model (simulatability), at the level of the individual components (e.g., parameters) (decomposability), and at the level of the training algorithm (algorithmic transparency). First, simulatability refers to contemplate the entire model at once and is satisfied in **SPSM** by it's nature of a sparse linear model, as produced by lasso regression Tibshirani (1996). Moreover, we claim that **SPSM** is small and simple (Rudin, 2019) , in that we allow a human to take the input data along with the parameters of the model and perform in a reasonable amount of time all the computations necessary to make a prediction in order to fully understand a model. The aspect of decomposabilty (Lipton et al., 2016)can be satisfied by using tabular data where features are intuitively meaningful. To that end, we use two real-world tabular data sets in the experiments and present the coefficient values for input features in Table 3. Moreover, one can choose to display the coefficients in a standardized or non-standardized way to provide even better insights. The comprehension of the coefficients depends also on domain knowledge. Finally, algorithmic transparency is given in **SPSM**, since in linear models, we understand the shape of the error surface and have some confidence that training will converge to a unique solution, even for previously unseen test data. Additionally, Henelius et al. (2017) claims that knowing interactions between two or more attributes makes a model more interpretable. **SPSM** shows in $\theta + \Delta$ the coefficient adaptation between the shared model and the pattern specific model and therefore reveals associations between attributes.

While the method presented is limited to learning linear models, it is not limited to learning from linear data generating processes. In fact, there are also many cases where the goal is to consider the best linear approximation to a nonlinear function given the risk of hold-out. We have presented a way to do this given patterns of missingness at test time. The restriction to linear models can be overcome by considering other classes of parametric models for which the class is closed under parameter addition. Although this technically includes neural network estimators (with fixed architecture), we do not expect linear combinations of model parameters to perform as well for them. An interesting direction for future work is to identify other classes of models developed with interpretability that might benefit from this type of sparsity (parameter sharing). Future work could include different regularization methods, such as adaptive LASSO or fitting separate regularization terms for each pattern, as well as quantitative analysis of variance reduction implied by parameter sharing.

Acknowledgement

Data collection and sharing was funded by ADNI (NIH #U01 AG024904) and DOD ADNI (#W81XWH-12-2-0012). ADNI is funded by the National Institute on Aging, the National Institute of Biomedical Imaging and Bioengineering, and through generous contributions from the following: AbbVie, Alzheimer's Association; Alzheimer's Drug Discovery Foundation; Araclon Biotech; BioClinica, Inc.; Biogen; Bristol-Myers Squibb Company; CereSpir, Inc.; Cogstate; Eisai Inc.; Elan Pharmaceuticals, Inc.; Eli Lilly and Company; EuroImmun; F. Hoffmann-La Roche Ltd and its affiliated company Genentech, Inc.; Fujirebio; GE Healthcare; IXICO Ltd.; Janssen Alzheimer Immunotherapy Research & Development, LLC.; Johnson & Johnson Pharmaceutical Research & Development LLC.; Lumosity; Lundbeck; Merck & Co., Inc.; Meso Scale Diagnostics, LLC.; NeuroRx Research; Neurotrack Technologies; Novartis Pharmaceuticals Corporation; Pfizer Inc.; Piramal Imaging; Servier; Takeda Pharmaceutical Company; and Transition Therapeutics. The Canadian Institutes of Health Research is providing funds to support ADNI clinical sites in Canada. Private sector contributions are facilitated by the Foundation for the National Institutes of Health (www.fnih.org). The grantee organization is the Northern California Institute for Research and Education, and the study is coordinated by the Alzheimer's Therapeutic Research Institute at the University of Southern California. ADNI data are disseminated by the Laboratory for Neuro Imaging at the University of Southern California.

LS and FJ are supported by the Wallenberg AI, Autonomous Systems and Software Program (WASP) funded by the Knut and Alice Wallenberg Foundation.

References

ADNI. Alzheimer’s Disease Neuroimaging Initiative, 2012. URL <http://adni.loni.usc.edu/wp-content/uploads/2013/09/DOD-ADNI-PM-12.7.12-FINAL.pdf>.

Yoshua Bengio and Francois Gingras. Recurrent neural networks for missing or asynchronous data. *Advances in neural information processing systems*, 8, 1995.

D. Bertsimas, A. Delarue, and J. Pauphilet. Prediction with Missing Data. *ArXiv*, abs/2104.03158, 2021.

Rohit Bhattacharya, Razieh Nabi, Ilya Shpitser, and James M Robins. Identification in missing data models represented by directed acyclic graphs. In *Uncertainty in Artificial Intelligence*, pages 1149–1158. PMLR, 2020.

Richard H Byrd, Peihuang Lu, Jorge Nocedal, and Ciyou Zhu. A limited memory algorithm for bound constrained optimization. *SIAM Journal on scientific computing*, 16(5):1190–1208, 1995.

James Carpenter and Michael Kenward. *Multiple imputation and its application*. John Wiley & Sons, 2012.

Zhengping Che, Sanjay Purushotham, Kyunghyun Cho, David Sontag, and Yan Liu. Recurrent neural networks for multivariate time series with missing values. *Scientific reports*, 8(1):1–12, 2018.

Tianqi Chen, Tong He, Michael Benesty, and Vadim Khotilovich. Package ‘xgboost’. *R version*, 90, 2019.

Nelson Cowan. The magical mystery four: How is working memory capacity limited, and why? *Current directions in psychological science*, 19(1):51–57, 2010.

Diane Dancer and Andrew Tremayne. R-squared and prediction in regression with ordered quantitative response. *Journal of Applied Statistics*, 32(5):483–493, 2005.

Dean De Cock. Ames, iowa: Alternative to the boston housing data as an end of semester regression project. *Journal of Statistics Education*, 19(3), 2011.

Morten W Fagerland, Stian Lydersen, and Petter Laake. Recommended confidence intervals for two independent binomial proportions. *Statistical methods in medical research*, 24(2):224–254, 2015.

Sarah Fletcher Mercaldo and Jeffrey D Blume. Missing data and prediction: the pattern submodel. *Biostatistics*, 21(2):236–252, 2020.

R. H. Groenwold, I. R. White, A. R. Donders, J. R. Carpenter, D. G. Altman, and K. G. Moons. Missing covariate data in clinical research: when and when not to use the missing-indicator method for analysis. *CMAJ : Canadian Medical Association journal = journal de l'Association medicale canadienne*, 184(11):1265–1269, 2012. doi: 10.1503/cmaj.110977.

JA Hanley and BJ McNeil. A method of comparing the areas under receiver operating characteristic curves derived from the same cases, 1983.

Andreas Henelius, Kai Puolamäki, and Antti Ukkonen. Interpreting classifiers through attribute interactions in datasets. *arXiv preprint arXiv:1707.07576*, 2017.

Kristel JM Janssen, Yvonne Vergouwe, A Rogier T Donders, Frank E Harrell Jr, Qingxia Chen, Diederick E Grobbee, and Karel GM Moons. Dealing with missing predictor values when applying clinical prediction models. *Clinical chemistry*, 55(5):994–1001, 2009.

Michael P Jones. Indicator and stratification methods for missing explanatory variables in multiple linear regression. *Journal of the American statistical association*, 91(433):222–230, 1996.

Diederik P Kingma and Jimmy Ba. Adam: A method for stochastic optimization. *arXiv preprint arXiv:1412.6980*, 2014.

William A Knaus, Frank E Harrell, Joanne Lynn, Lee Goldman, Russell S Phillips, Alfred F Connors, Neal V Dawson, William J Fulkerson, Robert M Califf, Norman Desbiens, et al. The support prognostic model: Objective estimates of survival for seriously ill hospitalized adults. *Annals of internal medicine*, 122(3):191–203, 1995.

Marine Le Morvan, Julie Josse, Thomas Moreau, Erwan Scornet, and Gaël Varoquaux. NeuMiss networks: differentiable programming for supervised learning with missing values. *arXiv:2007.01627*, 2020.

Marine Le Morvan, Julie Josse, Erwan Scornet, and Gaël Varoquaux. What's a good imputation to predict with missing values? *Advances in Neural Information Processing Systems*, 34, 2021.

Zachary C Lipton, David C Kale, Randall Wetzel, et al. Modeling missing data in clinical time series with rnns. *Machine Learning for Healthcare*, 56, 2016.

Roderick JA Little. Pattern-mixture models for multivariate incomplete data. *Journal of the American Statistical Association*, 88(421):125–134, 1993.

Roderick JA Little and Donald B Rubin. Statistical analysis with missing data, 1986.

Xiuming Liu, Dave Zachariah, and Petre Stoica. Robust prediction when features are missing. *IEEE Signal Processing Letters*, 27:720–724, 2020.

Benjamin M Marlin. *Missing Data Problems in Machine Learning*. PhD thesis, University of Toronto, 2008.

Guillermo Marshall, Bradley Warner, Samantha MaWhinney, and Karl Hammermeister. Prospective prediction in the presence of missing data. *Statistics in medicine*, 21(4):561–570, 2002.

Nicolai Meinshausen. Relaxed lasso. *Computational Statistics & Data Analysis*, 52(1):374–393, 2007.

George A Miller. The magical number seven, plus or minus two: Some limits on our capacity for processing information. *Psychological review*, 63(2):81, 1956.

Samaneh A Mofrad, Astri J Lundervold, Alexandra Vik, and Alexander S Lundervold. Cognitive and MRI trajectories for prediction of Alzheimer's disease. *Scientific Reports*, 11(1):1–10, 2021.

Marine Le Morvan, Nicolas Prost, Julie Josse, Erwan Scornet, and Gael Varoquaux. Linear predictor on linearly-generated data with missing values: non consistency and solutions. In Silvia Chiappa and Roberto Calandra, editors, *Proceedings of the Twenty Third International Conference on Artificial Intelligence*

and Statistics, volume 108 of *Proceedings of Machine Learning Research*, pages 3165–3174. PMLR, 26–28 Aug 2020. URL <https://proceedings.mlr.press/v108/morvan20a.html>.

Alfredo Nazabal, Pablo M Olmos, Zoubin Ghahramani, and Isabel Valera. Handling incomplete heterogeneous data using vaes. *Pattern Recognition*, 107:107501, 2020.

F. Pedregosa, G. Varoquaux, A. Gramfort, V. Michel, B. Thirion, O. Grisel, M. Blondel, P. Prettenhofer, R. Weiss, V. Dubourg, J. Vanderplas, A. Passos, D. Cournapeau, M. Brucher, M. Perrot, and E. Duchesnay. Scikit-learn: Machine Learning in Python. *Journal of Machine Learning Research*, 12:2825–2830, 2011.

Donald B Rubin. Inference and missing data. *Biometrika*, 63(3):581–592, 1976.

Cynthia Rudin. Stop explaining black box machine learning models for high stakes decisions and use interpretable models instead. *Nature Machine Intelligence*, 1(5):206–215, 2019.

Joseph L Schafer and John W Graham. Missing data: our view of the state of the art. *Psychological methods*, 7(2):147, 2002.

Shaun Seaman, John Galati, Dan Jackson, and John Carlin. What is meant by “missing at random”? *Statistical Science*, 28(2):257–268, 2013.

Robert Tibshirani. Regression shrinkage and selection via the lasso. *Journal of the Royal Statistical Society: Series B (Methodological)*, 58(1):267–288, 1996.

Volker Tresp and Thomas Briegel. A solution for missing data in recurrent neural networks with an application to blood glucose prediction. *Advances in Neural Information Processing Systems*, 10, 1997.

Stef Van Buuren. *Flexible Imputation of Missing Data (2nd ed.)*. Chapman and Hall/CRC, Boca Raton, FL, 2018. doi: <https://doi.org/10.1201/9780429492259>.

Pauli Virtanen, Ralf Gommers, Travis E Oliphant, Matt Haberland, Tyler Reddy, David Cournapeau, Evgeni Burovski, Pearu Peterson, Warren Weckesser, Jonathan Bright, et al. Scipy 1.0: fundamental algorithms for scientific computing in python. *Nature methods*, 17(3):261–272, 2020.

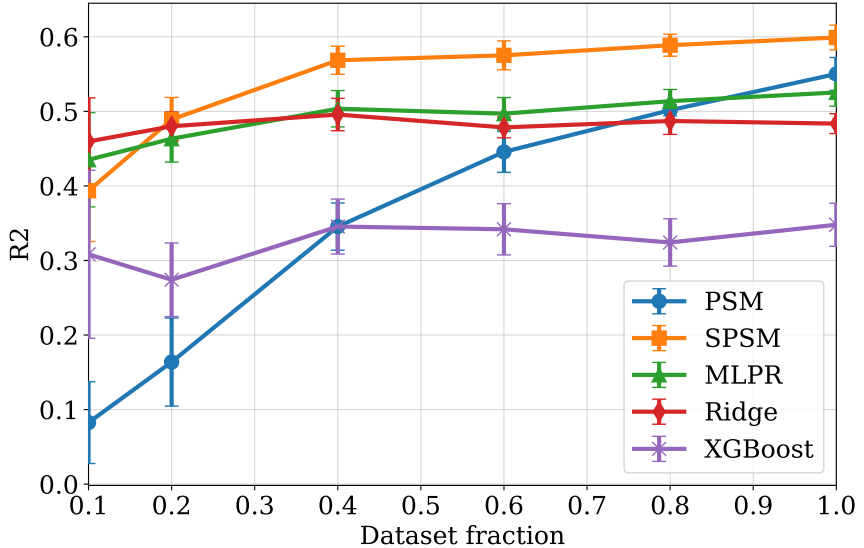


Figure 5: Performance on simulated data Setting B. Error bars indicate standard deviation over 5 random data splits. The complete dataset has $n = 4000$ samples.

A Proof of Example 1

Example 1 (Example 1 restated). *Assume that $X \sim \mathcal{N}(\mu, \Sigma)$ and that the outcome Y obeys (6)). Then, the Bayes-optimal predictor for an arbitrary missingness mask $m \in \mathcal{M}$, may be expressed as follows,*

$$f_m^* = \mathbb{E}[Y | X_{\neg m}, m] = (\theta_{\neg m} + \Delta_{\neg m}^*)^\top X_{\neg m} + C_m$$

where C_m is constant with respect to $X_{\neg m}$ and

$$\Delta_{\neg m}^* = (\Sigma_{\neg m, \neg m}^{-1})^\top \Sigma_{\neg m, m} \theta_m .$$

Proof. By properties of the multivariate Normal distribution, we have that

$$\begin{aligned} \mathbb{E}_{X_m}[X_m | X_{\neg m}] \\ = \mathbb{E}[X_m] + \Sigma_{m, \neg m} \Sigma_{\neg m, \neg m}^{-1} (X_{\neg m} - \mathbb{E}[X_{\neg m}]) \end{aligned}$$

and as a result, following the reasoning above,

$$\begin{aligned} \mathbb{E}[Y | X_{\neg m}] \\ = (\theta_{\neg m} + (\Sigma_{m, \neg m} \Sigma_{\neg m, \neg m}^{-1})^\top \theta_m)^\top X_{\neg m} + C_m \\ = (\theta_{\neg m} + \Delta_m^*)^\top X_{\neg m} + C_m, \end{aligned}$$

where $C_m = \mathbb{E}[X_m] + \Sigma_{m, \neg m} \Sigma_{\neg m, \neg m}^{-1} \mathbb{E}[X_{\neg m}] + \alpha_m$. \square

B Additional experimental results

B.1 Simulation results

Results for simulation Setting B can be found in Figure 5.

B.2 Real-world data sets

A figure illustrating the performance on SUPPORT with varying data set size is given in Figure 6. Table 4 presents the MSE score as an additional performance metric for the regression tasks using ADNI and SUPPORT data. For the non-MNAR setting in the SUPPORT data, we present the results for classification and regression tasks in Table 6 and Table 5. Moreover, the full table of pattern 4 non-zero coefficients with the corresponding missing features is displayed in Table 7.

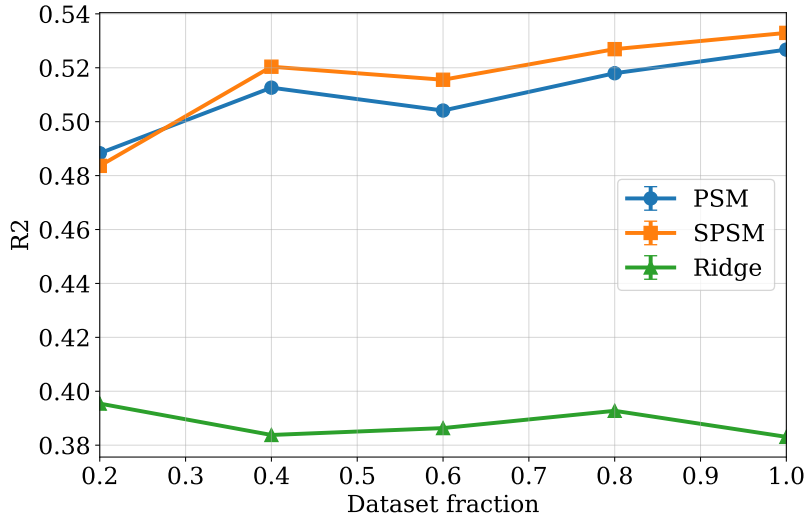


Figure 6: Performance on SUPPORT data for a regression task. Error bars indicate standard deviation over 5 random subsamples of the data.

Table 4: Experimental results of regression methods for ADNI and SUPPORT data set.

Linear Methods	MSE
<i>ADNI</i>	
Ridge, I_0	0.36 (0.26, 0.46)
XGB, I_μ	0.60 (0.48, 0.74)
MLP, I_μ	0.37 (0.27, 0.47)
PSM	0.50 (0.38, 0.62)
SPSM	0.35 (0.25, 0.45)
<i>SUPPORT</i>	
Ridge, I_0	0.61 (0.56, 0.66)
XGB, I_μ	0.69 (0.63, 0.75)
MLP, I_0	0.44 (0.39, 0.48)
PSM	0.47 (0.42, 0.52)
SPSM	0.47 (0.42, 0.51)

Table 5: Experimental results of regression methods for SUPPORT data set non-MNAR.

Regressions	R^2	MSE
<i>SUPPORT</i>		
Ridge, I_0	0.38 (0.34, 0.41)	0.62 (0.57, 0.67)
XGB, I_μ	0.27 (0.23, 0.31)	0.73 (0.67, 0.78)
MLP, I_0	0.55 (0.52, 0.58)	0.45 (0.40, 0.49)
PSM	0.51 (0.48, 0.54)	0.49 (0.44, 0.53)
SPSM	0.52 (0.49, 0.58)	0.47 (0.42, 0.51)

B.3 HOUSING data

The Ames Housing dataset (HOUSING) De Cock (2011) was compiled by Dean De Cock for use in data science education. The data set describing the sale of individual

Table 6: Experimental results of classifiers for SUPPORT data with non-MNAR.

Classifiers	AUC	Accuracy
SUPPORT		
LR, I_0	0.82 (0.80, 0.84)	0.75 (0.72, 0.78)
XGB, I_0	0.83 (0.81, 0.85)	0.76 (0.74, 0.78)
MLP, I_0	0.85 (0.84, 0.87)	0.78 (0.76, 0.81)
PSM	0.83 (0.81, 0.85)	0.78 (0.74, 0.80)
SPSM	0.83 (0.81, 0.85)	0.76 (0.73, 0.80)

Table 7: Full table showing Δ_m in the regression task using SPSM for ADNI.

Missing features in pattern 0:

		None			
No. of missingness pattern	Feature	Δ_m	θ	$\theta + \Delta_m$	
0	Age	-0.038	0.121	0.082	
	EDUCAT	0.014	-0.005	0.009	
	APOE4	0.046	-0.010	0.035	
	FDG	-0.032	-0.039	-0.071	
	ABETA	0.027	-0.000	0.027	
	LDELTOTAL	0.051	-0.391	-0.340	
	Entorhinal	0.007	-0.131	-0.124	
	ICV	0.013	0.093	0.106	
	Diagnose MCI	0.078	-0.139	-0.061	
	GEN Female	-0.054	0.003	-0.050	
	GEN Male	0.000	0.062	0.062	
	Not Hisp/ Latino	0.047	-0.114	-0.067	
	Married	0.115	-0.159	-0.044	

Missing features in pattern 1:

		FDG			
	1	Age	-0.052	0.121	0.069

Missing features in pattern 4:

ABETA, TAU and PTAU at baseline (bl)

		4	Age	-0.140	0.121	-0.019
		FDG	-0.090	-0.039	-0.129	
		Whole Brain	0.000	-0.045	-0.044	
		Fusiform	0.016	0.021	0.037	
		ICV	0.001	0.093	0.094	

Missing features in pattern 10:

FDG, ABETA (bl), TAU (bl), PTAU (bl)

10	APOE4	0.038	-0.010	0.027

residential property in Ames, Iowa from 2006 to 2010. The data set contains 2930 observations and a large number of explanatory variables (23 nominal, 23 ordinal, 14 discrete, and 20 continuous) involved in assessing home values. In this study we used a subset of the features 27 features to describe the main characteristics of a house. Examples of features included are measurements about the land ('LotFrontage', 'LotArea', 'LotShape', 'LandContour', 'LandSlope'), the 'Neighborhood', and 'HouseStyle', when the house was build ('YearBuilt'), or remodeled ('Year-

Table 8: A minimum sample size is required for SPSM to maintain predictive performance

Pattern number	Number of subjects per pattern	R^2
0	119	0.64 (0.53, 0.75)
1	30	0.30 (-0.10, 0.55)
6	27	0.71 (0.50, 0.92)
10	28	0.71 (0.50, 0.91)
others	≤ 13	undefined or insignificant

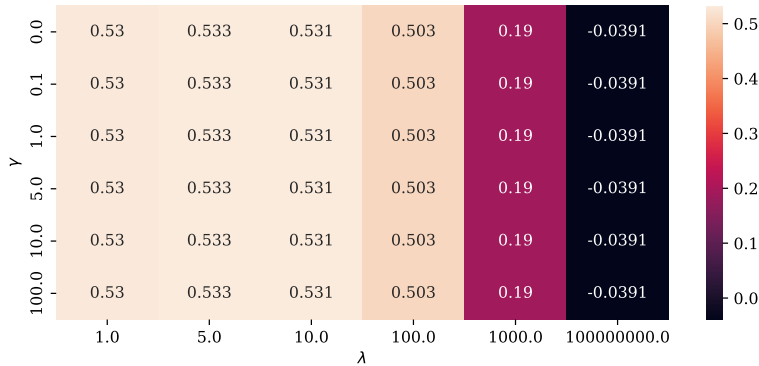


Figure 7: Heatmap visualising the tradeoff between interpretability and prediction power including different hyperparameter values for γ and λ , expressed by the R^2 using SUPPORT data. Each cell is indicating a γ, λ combination, e.g. 1,100 represents $1 = \gamma$ and $100 = \lambda$.

RemodAdd'). Moreover, features describing the outside of the house ('RoofStyle', 'Foundation'), technical equipment ('Heating', 'CentralAir', 'Electrical', 'KitchenAbvGr', 'Functional', 'Fireplaces', 'GarageType', 'GarageCars', 'PoolArea', 'Fence', 'MiscFeature'), and information about previous house selling prices and conditions ('MoSold', 'YrSold', 'SaleType', 'SaleCondition'). The numeric features were standardized and the categorical ones are one-hot-encoded during preprocessing. The HOUSING data set shows 15 different missingness pattern. An exploratory analysis has shown that the house sale prices are somehow skewed, which means that there is a large amount of asymmetry. Since the mean of the characteristic is greater than the median, it means that most houses were sold for less than the average price. In the classification predictions we look if the sale prices for a house are above or below the median, while for regression tasks we predict the sale price for a house.

We report the results of the HOUSING data set in Table 9. In classification, we see on average a high performance over all models, whereas the best performing one, XGB achieves an AUC of 0.96 and an accuracy of 0.91. SPSM achieves only slightly lower prediction power of 0.95 AUC and 0.88 accuracy than XGB. While LR, XGB and MLP depend on mean or zero imputation, PSM and SPSM are able to achieve comparable results without adding bias to their prediction with high confidence on average. For the HOUSING regression, the validation power suggested $\gamma = 10$, $\lambda = 100$ for SPSM, resulting in an R^2 of 0.64 and an MSE of 0.39. This result is better than for PSM (R^2 of 0.58 and MSE of 0.46) and thus demonstrates the benefit of coefficient sharing in SPSM compared to no sharing. Although Ridge, and MLP perform better the differences are only marginal to SPSM. The best performing model is the black-box method of XGB achieving an R^2 of 0.76 and MSE of 0.27 indicating the

Table 9: Experimental results of classification and regression methods for HOUSING data set.

Housing		
<i>Classification</i>	AUC	Accuracy
LR, I_μ	0.96 (0.94, 0.98)	0.90 (0.85, 0.95)
XGB, I_0	0.96 (0.94, 0.98)	0.91 (0.87, 0.96)
MLP, I_0	0.96 (0.93, 0.98)	0.90 (0.85, 0.94)
PSM	0.93 (0.90, 0.96)	0.88 (0.83, 0.93)
SPSM	0.95 (0.92, 0.97)	0.88 (0.83, 0.94)
<i>Regression</i>	R^2	MSE
Ridge, I_μ	0.68 (0.62, 0.75)	0.35 (0.25, 0.44)
XGB, I_0	0.76 (0.70, 0.81)	0.27 (0.18, 0.35)
MLP, I_0	0.64 (0.58, 0.71)	0.39 (0.29, 0.49)
PSM	0.58 (0.50, 0.65)	0.46 (0.35, 0.57)
SPSM	0.64 (0.57, 0.71)	0.39 (0.29, 0.49)

non-linearity of the data set.